GEOPHYSICS, VOL. 83, NO. 3 (MAY-JUNE 2018); P. Q15–Q24, 11 FIGS.
10.1190/GEO2017-0163.1

Correcting source and receiver scaling for virtual source imaging and monitoring

Andrey Bakulin[1], Dmitry Alexandrov[2], Christos Saragiotis[1], Abdullah Al Ramadan[1], and Boris Kashtan[2]

ABSTRACT

Virtual source redatuming is a data-driven interferometric approach that relies on constructive and destructive interference, and as a result it is quite sensitive to input seismic trace amplitudes. Land surveys are prone to amplitude changes that are unrelated to subsurface geology (source/receiver coupling, etc.). We have determined that such variations may be particularly damaging to construct a virtual-source signal for imaging and seismic monitoring applications, and they need to be correctly compensated before satisfactory images, repeatability, and proper relative amplitudes are achieved. We examine two methods to correct for these variations: a redatuming approach based on multidimensional deconvolution and multisurvey surface-consistent (SC) scaling. Using synthetic data, we discover that the first approach can only balance time-dependent variations between repeat surveys, e.g., compensate for variable shot scaling. In contrast, a multisurvey SC approach can compensate for shot and receiver scaling within each survey and among the surveys. As a result, it eliminates redatuming artifacts, brings repeat surveys to a common amplitude level, while preserving relative amplitudes required for quantitative interpretation of 4D amplitude differences. Applying an SC approach to a land time-lapse field data set with buried receivers from Saudi Arabia, we additionally conclude that separate SC scaling of early arrivals and deep reflections may produce better image and repeatability. This is likely due to the significantly different frequency content of early arrivals and deep reflections.

INTRODUCTION

Virtual source redatuming (Bakulin and Calvert, 2004) has been widely used to address various challenges in seismic imaging and monitoring (Bakulin et al., 2007). Many of the theoretical assumptions behind this method, such as the presence of sources on a closed surface all around the receivers, the placement of the sources in a homogeneous medium, and the absence of a free surface, are often violated in practice, particularly during land seismic acquisition. This does not invalidate the technique, but rather it requires specialized preprocessing that conditions the data in a way that gives the best chance for the redatuming to reconstruct the most important part of the Green's function (primary reflections in most cases). In this study, we specifically focus on the effects of space- and time-variant source and receiver scaling on prestack and poststack reflection amplitudes.

We emphasize that the virtual source method by crosscorrelation can handle natural or physics-based amplitude variations associated with wave propagation, such as transmission/reflection losses or geometric spreading, without any additional corrections. It cannot address amplitude fluctuations that are not related to the subsurface geology, such as variable source and receiver coupling. For example, the reduction in vibrator drive level (i.e., strength) near various field obstructions (such as wells, pipelines, buildings, and roads) results in variable shot strength.

We use synthetic modeling to demonstrate how variable time- and space-dependent source scaling can produce strong artifacts on the prestack virtual source gathers and make them poorly repeatable for monitoring. Incorrect scaling influences time-lapse virtual source data in three major ways:

1) It disrupts interferometric summation and leads to incorrect waveforms.

Manuscript received by the Editor 13 March 2017; revised manuscript received 26 October 2017; published ahead of production 09 January 2018; published online 23 February 2018.
[1]Saudi Aramco, Geophysics Technology, EXPEC Advanced Research Center, Dhahran, Saudi Arabia. E-mail: a_bakulin@yahoo.com; christos.saragiotis@gmail.com; abdallah.ramadan@aramco.com.
[2]Saint Petersburg State University, Saint Petersburg, Russia. E-mail: dalexl30@gmail.com; bmkashtan@gmail.com.

2) It distorts the relative amplitudes within each survey obtained on the resulting virtual source gathers and images.
3) Improper scaling that depends on vintage decreases repeatability of time-lapse data and masks the true 4D amplitude response among surveys.

For structural seismic imaging, it may be sufficient to address only the first shortcoming. For instance, automatic gain control (AGC) is a commonly accepted technique in land seismic processing to improve the interpretation of subsurface structure. If AGC is used with the same threshold for all surveys it can also force the amplitude level to be equal among surveys. However, AGC is a non-relative-amplitude-preserving process (Telford et al., 1990). As a result, any relative amplitude variation within, as well as between, the surveys cannot be trusted. In this study, we focus on time-lapse imaging using amplitude differences, and our goal is to find an approach that can address all three challenges mentioned above. Using synthetic data, we outline several possible solutions and analyze how they can mitigate these issues, quantify improvements in image and repeatability, and evaluate whether relative amplitudes are preserved. The first method is the intersurvey compensation scheme using multidimensional deconvolution (MDD) introduced by Alexandrov et al. (2015a, 2015b), who refer to it as deconvolution-convolution approach. This approach is an advanced virtual source technique based on MDD (Wapenaar et al., 2008), which provides a partial solution addressing mainly the third factor. It can effectively remove nonrepeatable differences between redatumed time-lapse gathers caused by variable source amplitudes, but it cannot correct for absolute source scalar variations present in both surveys. It is also unable to correct for different receiver scaling. The second approach uses multisurvey surface-consistent (SC) amplitude scaling, and it is expected to address all three challenges listed above. It recovers and corrects for source and receiver amplitude-scaling factors within the same survey, as well as between time-lapse surveys while preserving the relative amplitudes. In essence, the second approach is a generalized multisurvey version of the classical SC amplitude scaling (Taner and Koehler, 1981) that is essential for land seismic processing, which requires the preservation of relative amplitudes for tasks such as amplitude variation with offset inversion or any quantitative amplitude interpretation (Telford et al., 1990). We apply a multisurvey SC approach to field data using several different workflows and investigate the benefits of separate scaling of early arrivals and deep reflections.

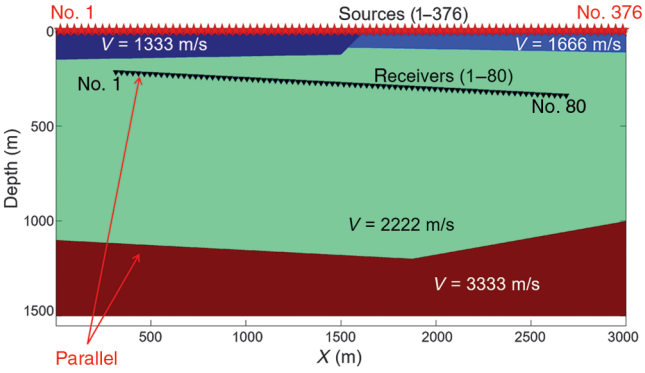

Figure 1. Acoustic model and acquisition geometry used for the synthetic test.

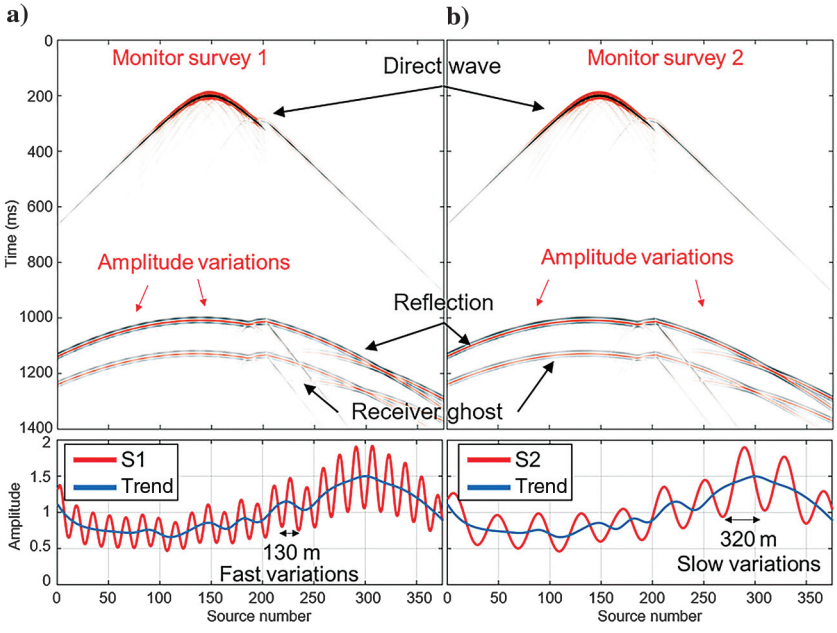

Figure 2. Common-receiver gathers of the (a) monitor survey one and (b) monitor survey two with their corresponding scaling factors S1 and S2.

SYNTHETIC EXAMPLES

To illustrate the effect of variable source and receiver scaling and evaluate possible solutions, we perform synthetic tests on a 2D time-lapse data set acquired with buried receivers (Figure 1) inspired by an actual field case study from Saudi Arabia (Bakulin et al., 2012). A single reflector is located at a depth of approximately 1100 m; the near surface comprises two low-velocity zones with $V = 1333$ m/s on the left part of the model and $V = 1666$ m/s on the right part (Figure 1). A dipping receiver line with 30 m spacing at a depth ranging from 216 to 340 m is parallel to the leftmost part of the target reflector. We simulate a surface vibrator shot line using 376 vertical-force sources with 7.5 m spacing. We did not introduce a free surface in the model to simplify the wavefield and track the prestack target reflection and associated artifacts caused by the source and receiver scaling without being obscured by ghost arrivals. First, we analyze the effect of shot scaling only and then we consider the general case when the sources and receivers are arbitrarily scaled.

Shot scaling

In this test, we modify the source amplitudes in two ways while keeping the receivers unscaled. Figure 2 shows a common-receiver gather for receiver 30 after source scaling along with the

corresponding amplitude-scaling factors. The three events on the seismogram are the direct wave, a reflection, and the receiver ghost arrival from the near-surface interface. We generate two monitor surveys using different source scaling whose values vary spatially with the high (S1) and low (S2) wavelength of 130 and 320 m, respectively. The blue line (Figure 2) indicates a background shot-amplitude trend. The spatially varying shot-amplitude oscillations can be observed on the reflection and ghost arrivals as ripples on a common-receiver gather.

For each pair of receivers $\mathbf{x}_B$ and $\mathbf{x}'_A$, the virtual source gather can be constructed according to the following equation (Bakulin and Calvert, 2004):

$$\hat{C}(\mathbf{x}_B, \mathbf{x}'_A; \omega) = \sum_s \hat{U}(\mathbf{x}_B, \mathbf{x}_S^{(s)}; \omega)\hat{U}^*_{\text{inc}}(\mathbf{x}'_A, \mathbf{x}_S^{(s)}; \omega), \quad (1)$$

where $\hat{U}(\mathbf{x}_B, \mathbf{x}_S; \omega)$ is the full wavefield at the receiver $\mathbf{x}_B$ and $\hat{U}^*_{\text{inc}}(\mathbf{x}'_A, \mathbf{x}_S; \omega)$ is the incident field at the receiver $\mathbf{x}'_A$, which is the location of the virtual source. $\hat{C}(\mathbf{x}_B, \mathbf{x}'_A; \omega)$ is often called a correlation function. The caret $\hat{}$ shows that the function is in the frequency domain, whereas the asterisk * indicates the complex conjugate. Stacking is performed over all sources $\mathbf{x}_S$. Because we are only interested in reflections in the virtual source data, we will use early arrivals as the $\hat{U}_{\text{inc}}(\mathbf{x}'_A, \mathbf{x}_S; \omega)$ component of correlation and reflection arrivals as $\hat{U}(\mathbf{x}_B, \mathbf{x}_S; \omega)$. Depending on the source coordinate, the shot scaling factors α_S affect the constructive and destructive interference as shown by this equation:

$$\hat{C}(\mathbf{x}_B, \mathbf{x}'_A; \omega) = \sum_s \alpha_S^2 \hat{U}(\mathbf{x}_B, \mathbf{x}_S^{(s)}; \omega)\hat{U}^*_{\text{inc}}(\mathbf{x}'_A, \mathbf{x}_S^{(s)}; \omega). \quad (2)$$

As a result, after redatuming, the source amplitude variations transform into artifacts visible on the common-receiver gathers shown in Figure 3a and 3b. The fast source-amplitude oscillations distort the reflection amplitudes on the virtual source gather and add noise before the reflection event (Figure 3a). The long-wavelength source amplitude variations introduce more subtle artifacts that appear like amplitude perturbations in the reflection strength along the target event (Figure 3b). We use the normalized root-mean-squared (NRMS) difference (see Kragh and Christie, 2002) to quantify the discrepancy between surveys. The NRMS is defined as

$$\text{NRMS}(\%) = 200\frac{\text{rms}(\text{tr}_1(t) - \text{tr}_2(t))}{\text{rms}(\text{tr}_1(t)) + \text{rms}(\text{tr}_2(t))}, \quad (3)$$

where $\text{tr}_1(t)$ and $\text{tr}_2(t)$ are the traces from different surveys. Then, we compute NRMS between the corresponding traces of the two surveys in the window containing the reflection and then find an average value. After redatuming, the average NRMS between the two monitor surveys is 48% (the difference between Figure 3a and 3b).

Intersurvey compensation scheme using MDD

One way to improve the repeatability during redatuming is to use the so-called deconvolution-convolution approach (Alexandrov et al., 2015a, 2015b) based on MDD (Wapenaar et al., 2008) that compensates for relative source strength and signature difference between surveys by equalizing downgoing fields between them (Appendix A). It involves deconvolution of the correlation function of one survey with the corresponding point-spread function (PSF) $\hat{\Gamma}$ written as

$$\hat{\Gamma}(\mathbf{x}_A, \mathbf{x}'_A; \omega) = \sum_s \hat{U}_{\text{inc}}(\mathbf{x}_A, \mathbf{x}_S^{(s)}; \omega)\hat{U}^*_{\text{inc}}(\mathbf{x}'_A, \mathbf{x}_S^{(s)}; \omega), \quad (4)$$

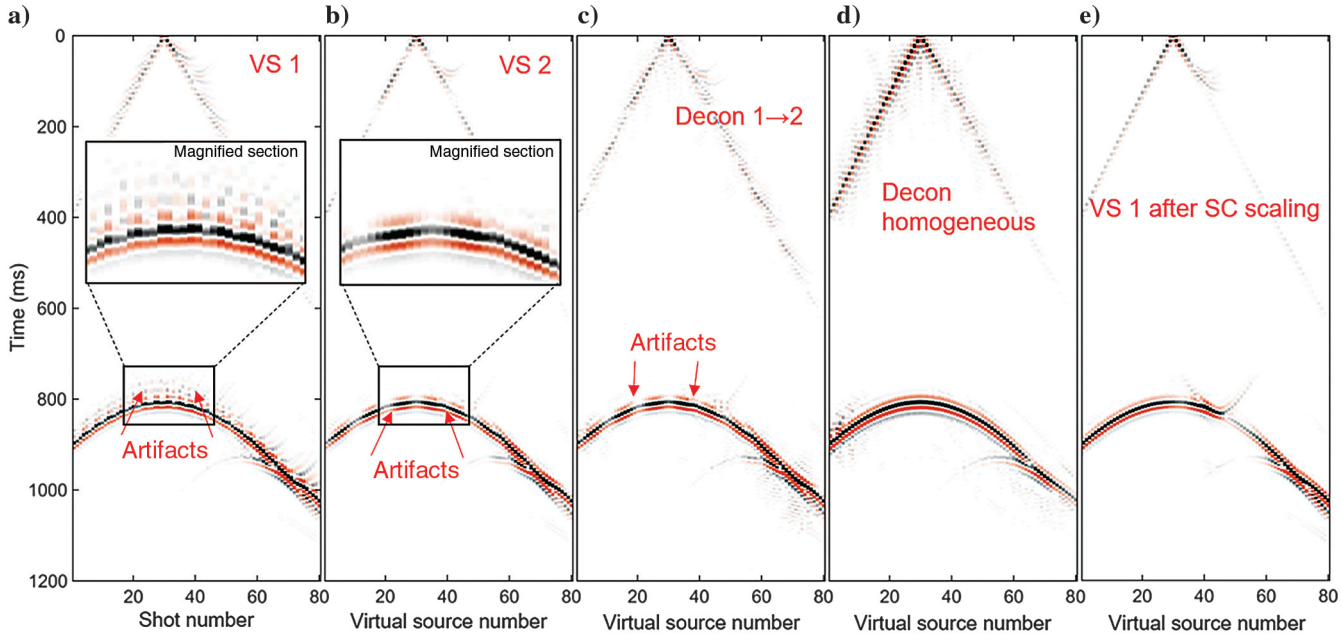

Figure 3. Common-receiver gathers for receiver 30 after redatuming using different approaches: virtual source redatuming of (a) survey one, (b) survey two, (c) deconvolution-convolution of survey one data using survey two as a reference, (d) deconvolution-convolution of survey one or two using homogeneous PSF, and (e) virtual source redatuming of the survey one after SC scaling using a shallow window with early arrivals.

and immediate convolution with the PSF of another survey used as a reference. The PSF defines the radiation pattern of the virtual source and absorbs the information about distortions caused by variable source scaling. The deconvolution-convolution approach can correct for different source strength and signatures between the surveys, and produce repeatable virtual source gathers. We compute the PSF in the frequency domain as the autocorrelation of the incident downgoing wavefield (equation 4). Figure 3c shows the result of the deconvolution-convolution approach applied to monitor survey one using survey two as a reference. The NRMS between reflections on the seismograms in Figure 3b and 3c is reduced to an average of 9%. Note that with this workflow we do not remove imaging artifacts associated with variations of the absolute source strength in each survey, but we rather replicate the same variations in the second survey as were present in the first survey; i.e., we replace the artifacts of redatumed survey one with the artifacts of survey two. One approach to restore more accurate amplitude scaling within each survey and suppress the imaging artifacts is to use synthetic reference PSFs for the convolution step computed in a homogeneous medium for both monitor surveys. In this case, the resulting gathers show better repeatability with an average NRMS of 6% as well as continuous reflectivity along the event without artifacts (Figure 3d). In the case of a complex near-surface environment, such an approach may create a potential mismatch between downgoing and upgoing wavefields.

Multisurvey SC scaling

An alternative approach is to extend the classical SC scaling to the 4D case with multiple surveys. Space-variant amplitude variations are best resolved by a least-squares error decomposition of the amplitudes into SC source and receiver scalars (Taner and Koehler, 1981). SC scaling removes space-variant amplitude changes that are not related to subsurface geology (source strength fluctuation, variable source/receiver coupling, etc.), and it is accepted as best industry practice for relative amplitude processing of land seismic data preceding any quantitative interpretation (Telford et al., 1990). Typically, the SC hypothesis represents the amplitude of each trace from the source n to the receiver m as a product of source, receiver, offset, and common-depth point (CDP) scalars (Taner and Koehler, 1981):

$$F_{nm} = S_n R_m Y_k D_l, \tag{5}$$

where $l = m - n$ and $k = (m + n)/2$. Using actual seismic amplitudes and applying the ln, the equality is then transformed into an overdetermined system of linear equations for the unknown factors $\ln(S)$, $\ln(R)$, $\ln(Y)$, and $\ln(D)$.

Here, we extend this approach to a multisurvey 4D case, in which all repeat surveys are solved together as a part of a global scaling exercise. For this purpose, sources occupying the same surface location, but coming from different surveys, are given different numbers. The same scheme is applied to the receivers, too. We then solve system 5 for the factors $\ln(S)$, $\ln(R)$, $\ln(Y)$, and $\ln(D)$, which now describe the amplitude scaling for the whole data set. This is to allow the source and the receiver to have different scalars for the same positions but restrict the offset and CDP to be position-invariant for all repeat surveys. We attempt not only to balance amplitudes within each survey (the goal of conventional SC scaling) but also between the surveys. Coupling surveys together allows us to bring them to a common amplitude level while allowing "local" or survey-specific scalars for shots and receivers to be different between repeat surveys. This addresses the real-world issue of variable or time-dependent coupling observed for sources (Jervis et al., 2012) and potentially receivers on land. We perform multisurvey SC scaling before redatuming and solve for source and receiver terms, and then we apply only shot scaling. In our tests, we use two different windows for SC scaling in which the algorithm will try to match the wavefields:

1) deep time window: 800–1700 ms over all offsets (reflections only)
2) shallow time window: 0–700 ms over offsets 0–250 m (early arrivals only).

Traditionally, a window is selected around reflected events after noise removal. Reflections are often weak compared with early arrivals and are obscured by remnants of unsuppressed noise. In these situations, using early arrivals with a higher signal-to-noise ratio can be a useful alternative.

Figure 4a and 4b shows the scaling factors obtained with the SC algorithm using a deep time window (blue) overlaid with the correct S1 and S2 factors (red). The scaling factors are recovered with good accuracy, and after the redatuming, the strong artifacts that we observe in Figure 3a are suppressed. The resulting gather without artifacts is visually indistinguishable from Figure 3d, and it is not shown here. Figure 4c shows that a multisurvey approach not only estimates space-variant scalars within each survey, but it also accurately reconstructs the source-amplitude ratio between the first and second surveys. This provides verification that the SC approach achieves its dual objective of balancing amplitudes within each survey and between multiple surveys.

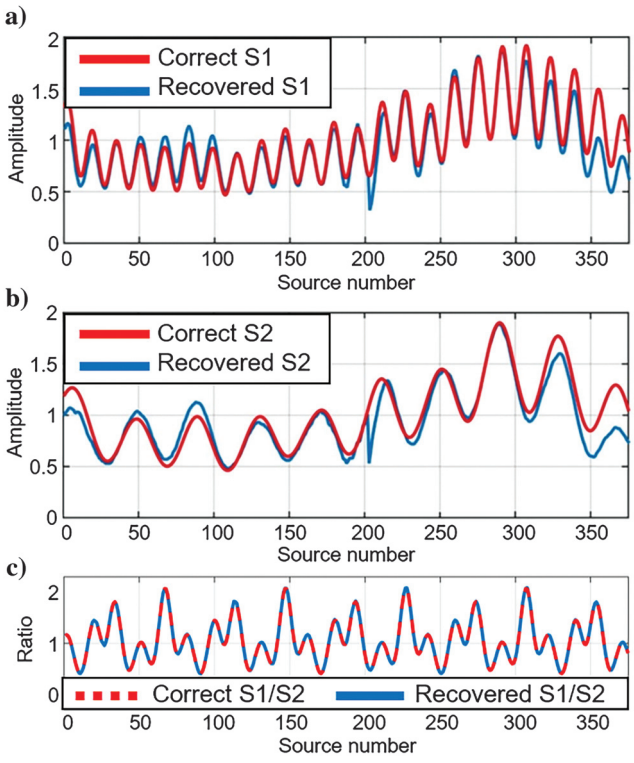

Figure 4. Shot scaling factors estimated using SC scaling with a deep time window for (a) survey one, (b) survey two, and (c) the ratio of the scaling factors.

For the shallow window, SC processing is able to estimate and compensate for the amplitude oscillations, but the actual amplitudes diverge from the S1 and S2 true scaling factors (Figure 5a and 5b). This is likely explained by the long-wavelength instability problem typical for such approaches (Wiggins et al., 1976); i.e., the estimation of the amplitude variations in terms of source and receiver components cannot be performed accurately over distances longer than a cable length. As a result, after redatuming, we eliminate short-wavelength imaging anomalies shown in Figure 3a and 3b, but we observe a discontinuity artifact on the target reflection arrival (Figure 3e). Nevertheless, the ratio between source scalars is estimated as accurately as for the deep reflection window (compare Figures 4c and 5c). This is confirmed by a reduction of the average NRMS between redatumed surveys to less than 1% for the deep and shallow time windows. This means that despite some instability in estimating long-wavelength scaling within the surveys and remaining imaging artifacts, the multisurvey approach with early arrivals accurately balances the amplitudes between repeat surveys enabling interpretation of 4D amplitude anomalies. The use of early arrivals may be attractive to successfully improve the repeatability of real data because this part of the data has much better signal-to-noise ratio compared with deep reflections.

Receiver scaling

We consider now a case in which changes in receiver coupling cause amplitude variations. These variations will not create artifacts (such as waveshape distortions and time shifts) on the virtual source gather because the virtual source gather is constructed for each pair of receivers independently (see equation 1). Instead, receiver amplitude variations will transform into different amplitude variations on the resulting virtual source gather. This happens because stacking is performed over all sources $\mathbf{x}_S$, and the scaling factors α_A and α_B that depend on the receiver coordinates $\mathbf{x}_A$ and $\mathbf{x}_B$ can be taken outside of the summation. As a result, wavefield correlation and summation over the sources will not suffer from space-variant receiver scaling. The result of this sum will be multiplied by a scaling factor $\alpha_A\alpha_B$, which depends on the location of the receiver $\mathbf{x}_B$ and virtual source $\mathbf{x}'_A$. As a consequence, after redatuming the data with modified receiver amplitudes, the virtual source gather embeds virtual source ($\mathbf{x}'_A$) and receiver ($\mathbf{x}_B$) variations according to the following equation:

$$\hat{C}(\mathbf{x}_B,\mathbf{x}'_A;\omega)=\alpha_A\alpha_B\sum_s \hat{U}(\mathbf{x}_B,\mathbf{x}_S^{(s)};\omega)\hat{U}^*_{\text{inc}}(\mathbf{x}'_A,\mathbf{x}_S^{(s)};\omega). \quad (6)$$

The intersurvey compensation scheme using MDD cannot correct variable receiver scaling because it targets the source signatures (Appendix A). As for the SC approach, there are two possible options to apply it:

1) correct receiver amplitudes before redatuming
2) perform redatuming and correct amplitudes of receivers and virtual sources on the redatumed data.

We perform another test in which shot and receiver amplitude scaling is applied to the data and we try to balance the amplitudes using SC scaling before redatuming. These surveys are referred to as surveys three and four. The corresponding input receiver-scaling factors R1 and R2 are presented in Figure 6 (red line), whereas the

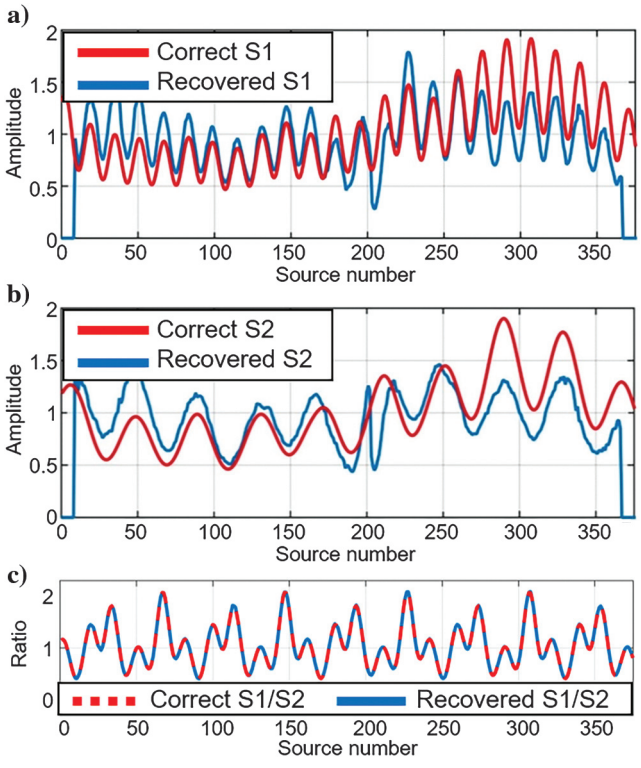

Figure 5. Shot scaling factors estimated using SC scaling with a shallow time window for (a) survey one, (b) survey two, and (c) the ratio of the scaling factors.

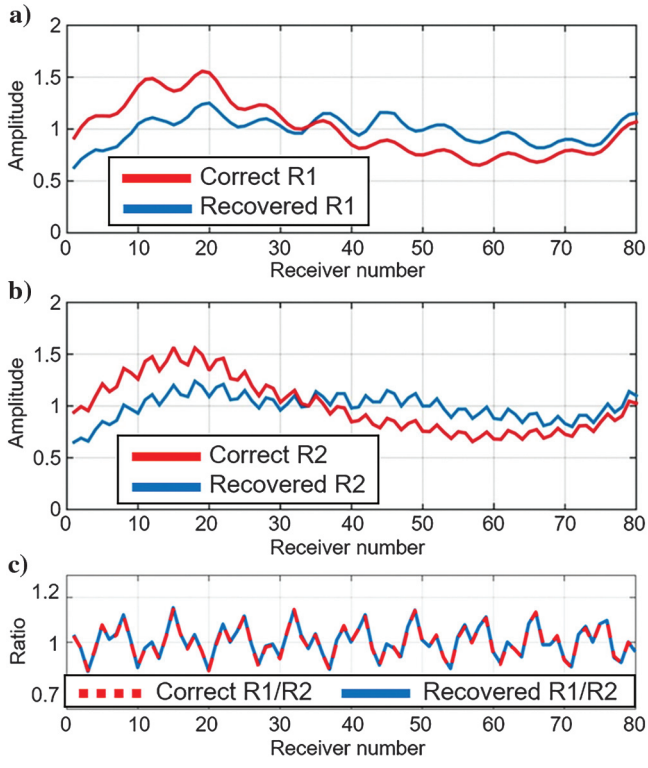

Figure 6. Receiver scaling factors estimated using SC scaling with a deep time window for (a) survey three, (b) survey four, and (c) the ratio of the scaling factors.

source-scaling factors remain the same as in the previous test. Note that for ease of interpretation, R1 and R2 are selected so that in monitor surveys, the receiver and source scalars have different oscillation frequencies. We apply the multisurvey SC approach, and we simultaneously estimate the source and receiver scalars for each survey using a deep time window (800–1700 ms). The estimated source-scaling factors (Figure 7) are as accurate as in the previous test (Figure 4). As for the receivers, although short-wavelength oscillations are estimated correctly, we observe a certain drift in the long-wavelength component (Figure 6) that is likely caused by the long-wavelength instability mentioned above (Wiggins et al., 1976). Nevertheless, the source-strength ratio between the two surveys is again accurately recovered (Figure 6c) suggesting that time-lapse balancing between surveys remains accurate. As in the previous case, this is confirmed by the average NRMS between surveys after redatuming not exceeding 1% for deep and shallow windows (not shown).

Based on the synthetic examples, we conclude that a multisurvey SC approach represents the most promising method that can remove space-variant amplitude changes that are not related to subsurface geology and also balance amplitudes between surveys for 4D analysis. This approach is easily extendable to more than two surveys and we demonstrate its application to real field data set.

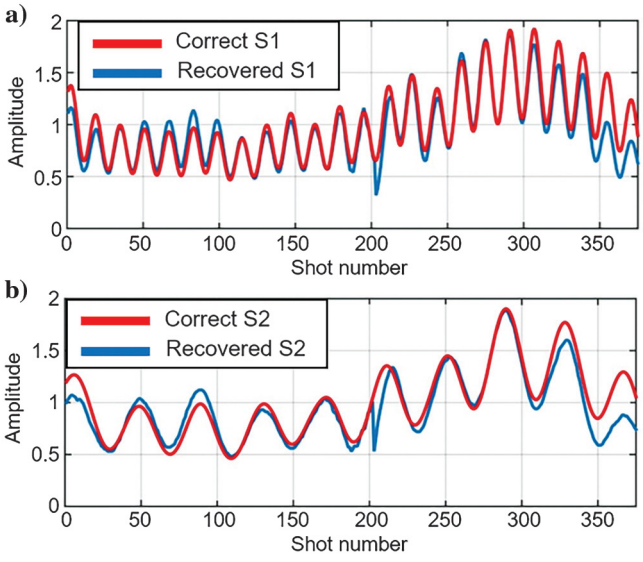

Figure 7. Shot scaling factors estimated using SC scaling with a deep time window for (a) survey three and (b) survey four.

FIELD EXAMPLE FROM SAUDI ARABIA

Alexandrov et al. (2015a, 2015b) recently report the application of a deconvolution-convolution approach on field data and demonstrate a significant improvement in repeatability compared with virtual source processing with simple crosscorrelation. Here, we use the same data (six repeated surveys from Saudi Arabia) to evaluate the effect of a multisurvey SC approach on imaging and repeatability. The acquisition setup (Figure 8) includes a single line of 80 receivers buried at 30 m depth and spaced at 30 m. A source carpet on the surface comprises nine shot lines, each with 300 shots and inline and crossline spacing of 7.5 m. The repeatability of this data acquired in a challenging desert environment suffers from various factors such as variable and time-dependent source coupling (Jervis et al., 2012).

The workflows applied to these data sets (Figure 9) have common preprocessing, redatuming, and stacking steps, but they differ in how the SC balancing was applied. Workflow one does not have SC scaling at all. In workflow two, we compute a single set of the source and receiver scalars for each survey using a time window over the target reflection arrival and apply them to reflections $\hat{U}(\mathbf{x}_B, \mathbf{x}_S; \omega)$ and early arrivals $\hat{U}^*_{\text{inc}}(\mathbf{x}'_A, \mathbf{x}_S; \omega)$. In workflow three, we apply scaling from the deep time gate to the reflections $\hat{U}(\mathbf{x}_B, \mathbf{x}_S; \omega)$ and we use separate scaling from a shallow time gate to correct the early arrivals $\hat{U}^*_{\text{inc}}(\mathbf{x}'_A, \mathbf{x}_S; \omega)$. Finally, workflow four includes all the steps of workflow three and includes additional SC balancing after redatuming. Note, that in all workflows we are doing multisurvey SC scaling to balance the amplitudes within the surveys, as well as across all survey vintages to bring the amplitudes to a common level. The workflow variations above are introduced to additionally handle effects that were not present in the synthetic data as explained below.

We use the described workflows to process six surveys from the acquisition shown in Figure 8. Figure 10a–10d shows the resulting CDP stacks for survey one. The red arrow indicates the target reflector. The bottom row (Figure 10e–10h) shows the corresponding CDP stacks with AGC applied before final stacking

Figure 11 shows the "return time curves" for repeatability (Bakulin et al., 2014) comprising NRMS for all pairs of surveys, one for each workflow in the same order as in Figure 10. Each point in Figure 10e–10h represents the NRMS value for a corresponding pair of surveys. NRMS is computed on stacked sections over the reservoir window after processing with a specific workflow. The return time curve is a best-fit straight line to the measured NRMS values.

With workflow one, we obtain the worst image quality and repeatability (Figures 10a and 11a), the image being unbalanced with high energy concentrated in traces with CDP numbers greater than 110, whereas the target event is very weak. Introducing the same SC balancing for early arrivals and deep reflections, the second workflow significantly improves the image balancing and makes the target reflector visible (Figures 10b and 11b). Repeatability for most of the combinations of surveys remains poor. We achieve much better results when we scale the early arrivals and

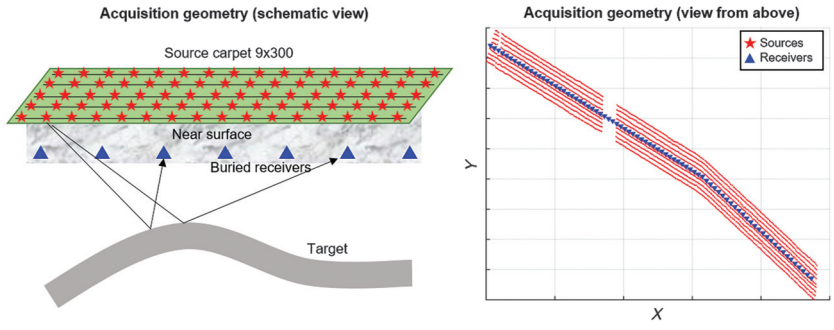

Figure 8. Acquisition geometry for the field 2D data set with 80 buried sensors at a 30 m depth from one of the onshore sites in Saudi Arabia.

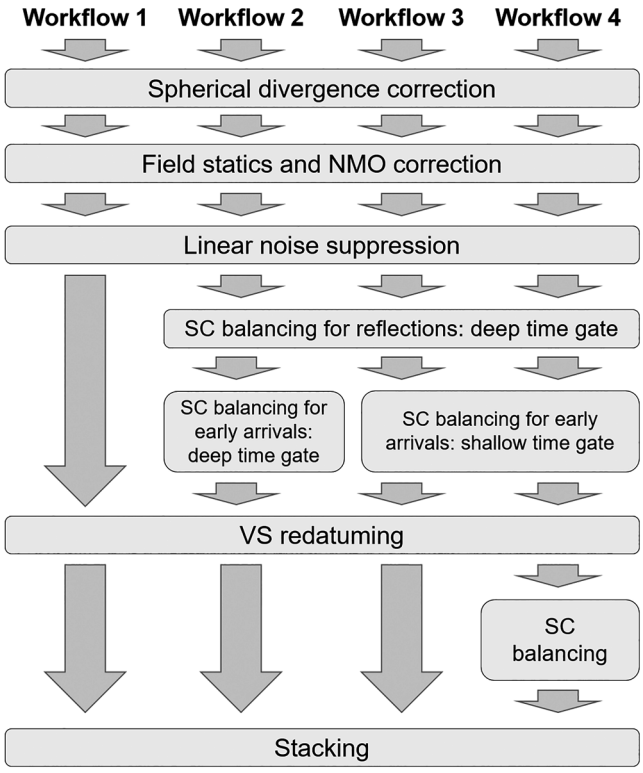

Figure 9. Processing workflows evaluated for the virtual source field data. Workflows differ in the SC processing step: Workflow one does not have this step; in workflow two, we apply the same SC balancing to early arrivals and deep reflections; in workflows three and four, we scale early arrivals with different scaling factors; and workflow four has an additional SC balancing step after virtual source redatuming.

reflections separately during the third workflow; the target event becomes more continuous and repeatable (Figures 10c and 11c). Additional SC balancing after redatuming in workflow four introduces subtle image improvements and reduces NRMS by 1%–2% on average compared with workflow three (Figures 10d and 11d).

Observe how workflow three performs significantly better than workflow two (Figure 10b and 10c). One possible explanation of such behavior could be variation of the centroid frequency with depth (time) due to the intrinsic attenuation (Hauge, 1981; Quan and Harris, 1993). Early arrivals have a significantly higher centroid frequency than deeper reflections, which results in different sets of scaling factors. Retailleau et al. (2014) report that frequency-dependent scaling of reflections alone can lead to better balanced images and improved reconstruction of the lower frequencies. In our case, the difference between the early arrivals and the deep reflections is more disparate, suggesting that the scaling between them may be quite different. Although we may not fully understand these effects, the field data clearly suggest that some additional factors are at play that we may need to address via separate scaling of early and late arrivals.

For comparison, we also show images and return curves for all workflows using AGC (Figures 10e–10h and 11e–11h). Here, AGC is used as a simple nonamplitude preserving process that allows us to obtain a robust structural image with pretty much any of the scaling workflows. Although structurally all images look similar after AGC, their relative amplitudes cannot be trusted because they are obtained by arbitrary trace-by-trace and sample-by-sample scaling within and between the surveys. We achieve similar or better results using the multisurvey SC approach based on clear physical principles and fully using the redundancy in the data. We confirm that the generalized multisurvey SC balancing extended to the 4D case with multiple surveys delivers improved virtual sources images and repeatability for challenging land buried receiver data.

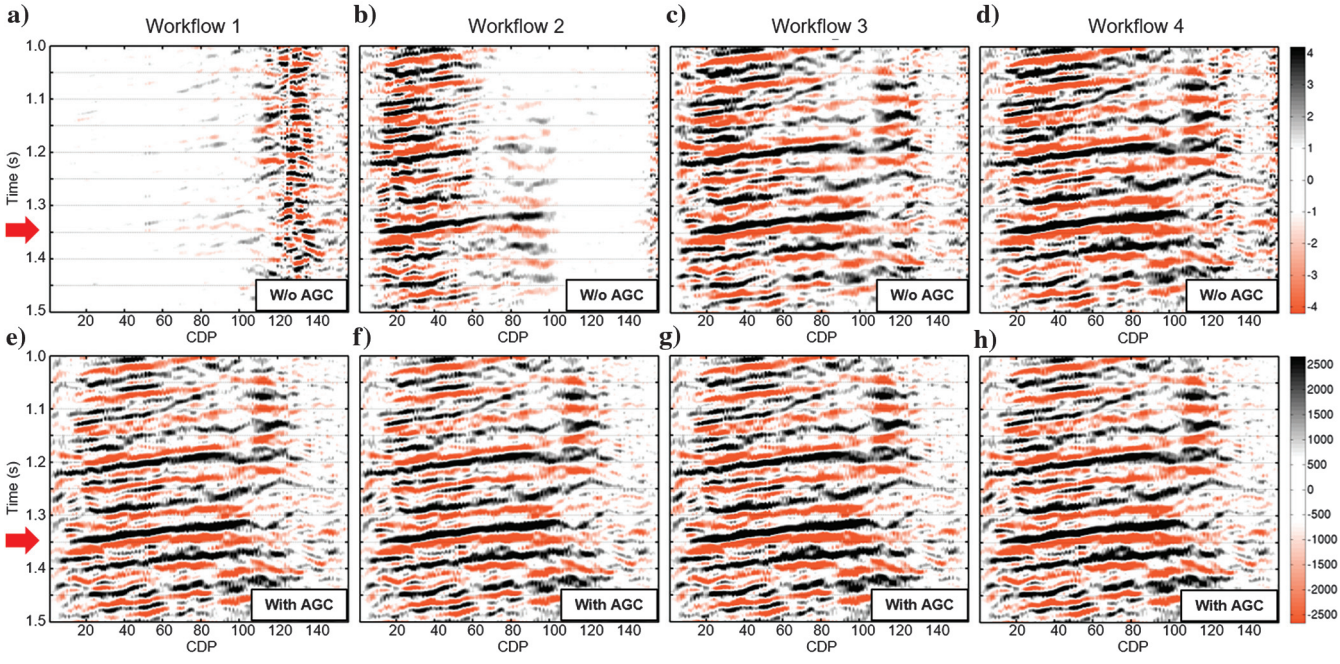

Figure 10. CDP stacks obtained after processing according to (a) workflow one, (b) workflow two, (c) workflow three, (d) workflow four, and (e-h) the same stacks with additional AGC applied.

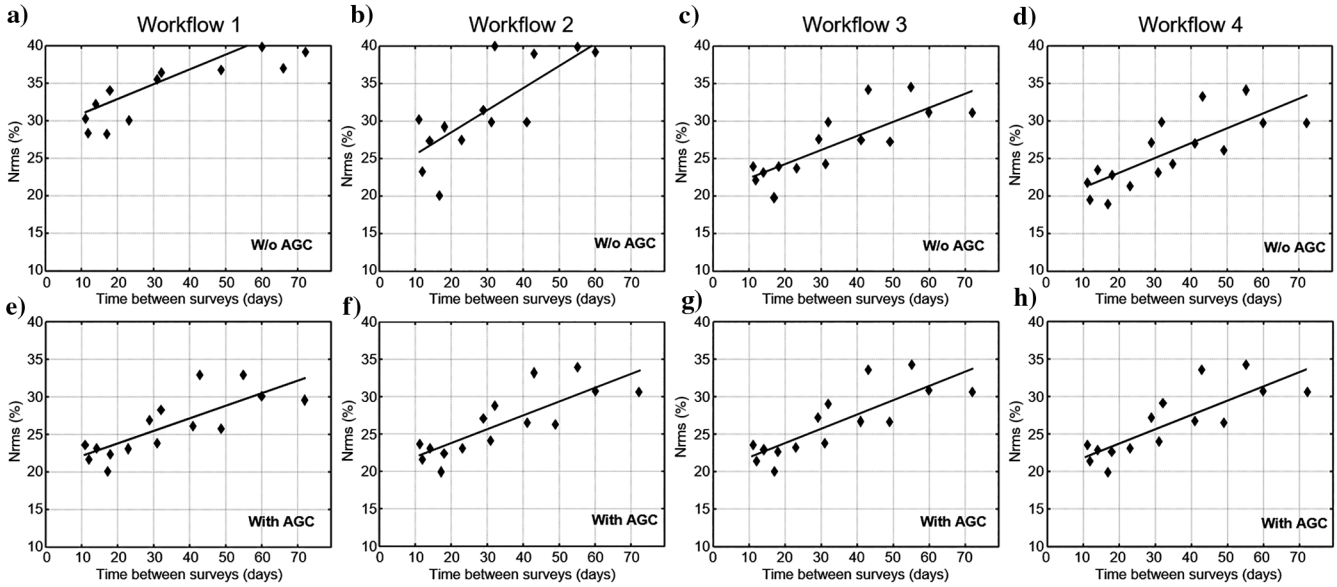

Figure 11. Return time curve for repeatability with NRMS between all pairs of CDP stacks obtained after processing according to (a) workflow one, (b) workflow two, (c) workflow three, (d) workflow four, and (e-h) the same pairs with additional AGC step.

In addition to variable coupling, land 4D surveys can also suffer from changing source signatures associated with the seasonal or permanent variations in the near surface (Bakulin et al., 2014). In the presence of variable coupling and source signatures, we advocate using the multisurvey SC scaling first to remove the effects of variable scaling followed up by MDD to compensate for variable source signatures as shown by Alexandrov et al. (2015a, 2015b).

CONCLUSION

We have identified that incorrect source and receiver scaling influences the time-lapse virtual source data in three major ways. First, the delicate balance of constructive and destructive interference is violated during the interferometric summation leading to artifacts on the redatumed data. Second, it distorts the relative amplitudes obtained in the resulting virtual source gathers and images. Third, improper time-dependent scaling can decrease the repeatability of time-lapse data and mask the true 4D amplitude response between surveys. Although the second and third factors are well-known for land 4D seismic, the first is unique for interferometric approaches such as virtual source redatuming. Although there are practical approaches for noise interferometry such as AGC or energy normalization aiming to reduce redatuming artifacts, they are only suitable for qualitative interpretation. This is analogous to use of AGC in land seismic processing that is only acceptable for structural imaging. For any quantitative interpretation, all three challenges should be addressed using amplitude-preserving approaches. We examine the effects of source and receiver scaling on the virtual source 4D imaging, propose such an amplitude-preserving approach and verify it on synthetic and real data.

We observe that variable shot scaling is particularly damaging for virtual source retrieval by crosscorrelation because it directly disrupts the constructive and destructive interference during redatuming and introduces artifacts manifested as amplitude distortions in the case of long-wavelength spatial variations and noise events for variations at a smaller spatial scale. Differences in shot strength and signatures between repeat surveys can be effectively compensated by intersurvey compensation scheme using MDD or deconvolution-convolution approach that uses one of the surveys as a reference during the convolution step. However, this technique cannot remove scaling-induced imaging artifacts in the reference survey, but rather it makes the artifacts in all other surveys to mimic the artifacts of the baseline. Such artifacts would lead to incorrect relative amplitudes within each survey and distort the interpretation. To properly balance the amplitudes within each survey, while maintaining a good image and repeatability, we modify this approach to use a reference PSF, computed for a homogeneous replacement of the near surface.

As for receiver scaling, it appears less damaging because it does not introduce artifacts to the interferometric redatuming per se, but rather causes amplitude variations of sources and receivers on the virtual source gathers. The intersurvey compensation scheme using MDD cannot address this issue. Therefore, we suggest correcting the receiver amplitudes before and after redatuming using more comprehensive approach that extends classical SC scaling to the 4D case with arbitrary number of repeat surveys. By combining all surveys in a single inversion, we enable not only balancing of amplitudes within each survey but also reconciling all of them to a common amplitude level. We have shown on synthetic tests that this provides a reasonable estimate of local source and receiver scalars for all surveys at once. These local or survey-specific scalars are different for each survey reflecting the variable and time-dependent nature of the source and receiver coupling on land in the presence of seasonal variations.

We apply the multisurvey SC approach to six time-lapse seismic field surveys acquired with permanently buried receivers in Saudi Arabia. The multisurvey SC approach delivers consistent amplitude level across all surveys thus enabling time-lapse interpretation, while compensating for strong space-variant fluctuations within each survey to deliver good redatumed images without artifacts. We achieve the best results in imaging and repeatability when we balance early arrivals and deep reflections separately, probably because of significantly different frequency contents between the

two. Multisurvey surface-consistent scaling is an amplitude-preserving approach that can effectively address all three challenges for time-lapse virtual source data. It is a natural extension of conventional SC scaling, and it is therefore recommended for 4D processing and imaging of land seismic data with or without redatuming.

ACKNOWLEDGMENT

We thank Saudi Aramco for support and permission to publish this work.

APPENDIX A

INTERFEROMETRIC REDATUMING

The virtual source by crosscorrelation is a redatuming technique that creates a virtual shot at the position of one of the receivers that can be used for imaging and time-lapse monitoring with permanent receivers. This technique uses experimentally measured Green's functions from buried receivers and as such does not require knowledge of any velocity model (Bakulin and Calvert, 2004). The method involves crosscorrelation of the full wavefield $U(\mathbf{x}_B, \mathbf{x}_S^{(s)}; t)$ at the receiver $\mathbf{x}_B$ with the incident $U_{\text{inc}}(\mathbf{x}'_A, \mathbf{x}_S^{(s)}; t)$ at the receiver $\mathbf{x}'_A$ and stacking over all sources $\mathbf{x}_S$:

$$\hat{C}(\mathbf{x}_B, \mathbf{x}'_A; \omega) = \sum_s \hat{U}(\mathbf{x}_B, \mathbf{x}_S^{(s)}; \omega)\hat{U}^*_{\text{inc}}(\mathbf{x}'_A, \mathbf{x}_S^{(s)}; \omega). \quad \text{(A-1)}$$

Here, the caret indicates the frequency domain. The correlation function $\hat{C}(\mathbf{x}_B, \mathbf{x}'_A; \omega)$ is usually interpreted as a wavefield generated by the source at the position $\mathbf{x}_B$ and registered by the receiver $\mathbf{x}'_A$. The derivation of this relation required several assumptions that are often violated in field experiments. In particular, the method assumes the absence of a free surface or any reflection from above the source level as well as full aperture of sources around the receivers. Although both of these assumptions are usually violated, up-down wavefield separation (Mehta et al., 2007) can help to avoid spurious events on the redatumed gather in practice. However, if the medium, that generates spurious events, as well as the locations of sources and receivers, remain constant from survey to survey these artifacts will remain repeatable. Therefore, image distortions in this case will pose little direct problem to seismic monitoring even if up-down separation is unavailable.

Another assumption is that all sources have exactly the same wavelet shape. When this is not fulfilled, the radiation pattern of the virtual source becomes distorted. Even though the redatumed image will be altered, as long as the source wavelets remain constant from survey to survey, the redatumed gathers will remain repeatable. This may happen, for instance, when source coupling depends strongly on the position of the source but does not vary with time.

A deeper insight into the correlation function is given by a relationship, used in MDD (Wapenaar and Van der Neut, 2011):

$$\hat{C}(\mathbf{x}_B, \mathbf{x}'_A; \omega) = \int_{\partial \mathbf{D}} \hat{X}(\mathbf{x}_B, \mathbf{x}_A; \omega)\hat{\Gamma}(\mathbf{x}_A, \mathbf{x}'_A; \omega)d\mathbf{x}_A. \quad \text{(A-2)}$$

Here, integration is performed over the receiver array on the boundary $\partial\mathbf{D}$ in the subsurface, $\hat{X}$ is the subsurface reflection response, depending solely on the properties of the medium, $\hat{\Gamma}$ is the PSF:

$$\hat{\Gamma}(\mathbf{x}_A, \mathbf{x}'_A; \omega) = \sum_s \hat{U}_{\text{inc}}(\mathbf{x}_A, \mathbf{x}_S^{(s)}; \omega)\hat{U}^*_{\text{inc}}(\mathbf{x}'_A, \mathbf{x}_S^{(s)}; \omega). \quad \text{(A-3)}$$

Using equation A-2, we can interpret the correlation function $\hat{C}$ as the reflection response of the media $\hat{X}$ blurred by the PSF $\hat{\Gamma}$. In other words, the PSF $\hat{\Gamma}$ defines the waveshape and radiation pattern of the virtual sources obtained with crosscorrelation. Traditional MDD involves deconvolving the PSF from the correlation function. This can improve the image and remove spurious events related to the free surface and incomplete source aperture as well as distortions caused by source wavelet variations and attenuation. However, inversion of the matrix $\hat{\Gamma}$ can generate undesired artifacts and deteriorate rather than improve the repeatability, especially when the receiver spacing is not dense enough for stable inversion. For this reason, we take an alternative approach that aims to improve the repeatability of the virtual source data by assigning a common source wavelet to each survey, while leaving the imprint of the free-surface multiples and other near-surface effects.

Let us consider two surveys, indicated by superscripts $i = 0$ and $i = 1$, respectively. For both surveys we can compute a correlation function $\hat{C}^{(i)}$ and a PSF $\hat{\Gamma}^{(i)}$. As noted before, the correlation function is classically interpreted as redatumed data. Alternatively, we can interpret these correlation functions as

$$\hat{C}^{(i)}(\mathbf{x}_B, \mathbf{x}'_A; \omega) = \int_{\partial \mathbf{D}} \hat{X}^{(i)}(\mathbf{x}_B, \mathbf{x}_A; \omega)\hat{\Gamma}^{(i)}(\mathbf{x}_A, \mathbf{x}'_A; \omega)d\mathbf{x}_A, \quad \text{(A-4)}$$

where $\hat{X}^{(i)}$ is the subsurface reflection response. From this representation, it is clear that the change in the correlation function $\hat{C}^{(i)}$ describes the changes in the reflection response $\hat{X}^{(i)}$ only when the PSF $\hat{\Gamma}^{(i)}$ is repeatable. If $\hat{\Gamma}^{(1)} \neq \hat{\Gamma}^{(0)}$, theoretically we can improve the repeatability by MDD, removing the PSF from the redatumed data. However, inversion instability can lead to additional artifacts. To overcome this issue, we convolve the retrieved reflection responses $\hat{X}^{(0)}$ and $\hat{X}^{(1)}$ with another PSF $\hat{\Gamma}^{(b)}$, where superscript b stands for "base." We can choose one of the surveys as a baseline, or use an average PSF for all surveys. Alternatively, we can construct the base PSF via synthetic modeling using a simplified replacement media between the source and receiver. Effectively, we apply a filter that is based on the ratio of two PSFs to the correlation function.

In the case of source amplitude variations only, the PSF will be affected in the right side of equation A-4 because the subsurface response $\hat{X}^{(i)}$ does not depend on the physical sources $\mathbf{x}_S$. When the receiver strength is varying, this also affects the reflection response $\hat{X}^{(i)}$. Therefore, deconvolving $\hat{\Gamma}^{(i)}$ from the correlation function $\hat{C}^{(i)}$ will not completely remove the effect of such variations.

REFERENCES

Alexandrov, D., J. Van der Neut, A. Bakulin, and B. Kashtan, 2015a, Improving repeatability of land seismic data using virtual source approach based on multidimensional deconvolution: 77th Annual International Conference and Exhibition, EAGE, Extended Abstracts, doi: 10.3997/2214-4609.201412558.

Alexandrov, D., J. Van der Neut, A. Bakulin, and B. Kashtan, 2015b, Correcting for non-repeatable source signatures in 4D seismic with buried receivers: Virtual source case study from Saudi Arabia: 85th Annual International Meeting, SEG, Expanded Abstracts, 5343–5347, doi: 10.1190/segam2015-5890959.1.

Bakulin, A., R. Burnstad, M. Jervis, and P. Kelamis, 2012, Evaluating permanent seismic monitoring with shallow buried sensors in a desert envi-

ronment: 82nd Annual International Meeting, SEG, Expanded Abstracts, doi: 10.1190/segam2012-0951.1.
Bakulin, A., and R. Calvert, 2004, Virtual source: New method for imaging and 4D below complex overburden: 74th Annual International Meeting, SEG, Expanded Abstracts, 2477–2480, doi: 10.1190/1.1845233.
Bakulin, A., A. Mateeva, K. Mehta, P. Jorgensen, I. Sinha Herhold, and J. Lopez, 2007, Virtual source applications to imaging and reservoir monitoring: The Leading Edge, **26**, 732–740, doi: 10.1190/1.2748490.
Bakulin, A., R. Smith, M. Jervis, and R. Burnstad, 2014, Near surface changes and 4D seismic repeatability in desert environment: From days to years: 84th Annual International Meeting, SEG, Expanded Abstracts, 4843–4847, doi: 10.1190/segam2014-0429.1.
Hauge, P. S., 1981, Measurements of attenuation from vertical seismic profiles: Geophysics, **46**, 1548–1558, doi: 10.1190/1.1441161.
Jervis, M., A. Bakulin, R. Burnstad, C. Berron, and E. Forgues, 2012, Suitability of vibrators for time-lapse monitoring in the Middle East: 82nd Annual International Meeting, SEG, Expanded Abstracts, doi: 10.1190/segam2012-0948.1.
Kragh, E., and P. Christie, 2002, Seismic repeatability, normalized rms, and predictability: The Leading Edge, **21**, 640–647, doi: 10.1190/1.1497316.
Mehta, K., A. Bakulin, J. Sheiman, R. Calvert, and R. Snieder, 2007, Improving the virtual source method by wavefield separation: Geophysics, **72**, no. 4, V79–V86, doi: 10.1190/1.2733020.
Quan, Y., and J. M. Harris, 1993, Seismic attenuation tomography based on centroid frequency shift: 63rd Annual International Meeting, SEG, Expanded Abstracts, 41–44, doi: 10.1190/1.1822504.
Retailleau, M., R. El Asrag, and J. Shorter, 2014, Processing land broadband data: Challenges that Oman surveys present and how they are addressed: Presented at the EAGE/SPG Workshop on Broadband Seismic, Session: Broadband OBC & Land, doi: 10.3997/2214-4609.20141699.
Taner, M. T., and F. Koehler, 1981, Surface consistent corrections: Geophysics, **46**, 17–22, doi: 10.1190/1.1441133.
Telford, W. M., L. P. Geldart, and R. E. Sheriff, 1990, Applied geophysics: Cambridge University Press.
Wapenaar, K., and J. Van der Neut, 2011, Seismic interferometry by crosscorrelation and by multidimensional deconvolution: A systematic comparison: Geophysical Journal International, **185**, 1335–1364, doi: 10.1111/j.1365-246X.2011.05007.x.
Wapenaar, K., J. van der Neut, and E. Ruigrok, 2008, Passive seismic interferometry by multidimensional deconvolution: Geophysics, **73**, no. 6, A51–A56, doi: 10.1190/1.2976118.
Wiggins, R. A., K. L. Larner, and R. D. Wisecup, 1976, Residual statics analysis as a general linear inverse problem: Geophysics, **41**, 922–938, doi: 10.1190/1.1440672.